technologies

MDPI

Review

Recent Advances in Si-Compatible Nanostructured Photodetectors

Rahaf Douhan, Kirill Lozovoy *, Andrey Kokhanenko, Hazem Deeb, Vladimir Dirko and Kristina Khomyakova

Faculty of Radiophysics, National Research Tomsk State University, Lenin Av. 36, 634050 Tomsk, Russia
* Correspondence: lozovoymailbox@gmail.com

Abstract: In this review the latest advances in the field of nanostructured photodetectors are considered, stating the types and materials, and highlighting the features of operation. Special attention is paid to the group-IV material photodetectors, including Ge, Si, Sn, and their solid solutions. Among the various designs, photodetectors with quantum wells, quantum dots, and quantum wires are highlighted. Such nanostructures have a number of unique properties, that made them striking to scientists' attention and device applications. Since silicon is the dominating semiconductor material in the electronic industry over the past decades, and as germanium and tin nanostructures are very compatible with silicon, the combination of these factors makes them the promising candidate to use in future technologies.

Keywords: photodetector; quantum well; quantum dot; silicon; germanium; tin

Citation: Douhan, R.; Lozovoy, K.; Kokhanenko, A.; Deeb, H.; Dirko, V.; Khomyakova, K. Recent Advances in Si-Compatible Nanostructured Photodetectors. *Technologies* **2023**, *11*, 17. https://doi.org/10.3390/technologies11010017

Academic Editor: Petra Paiè

Received: 20 December 2022
Revised: 16 January 2023
Accepted: 21 January 2023
Published: 24 January 2023

1. Introduction

During the last century, light detection methods have improved significantly, from thermal detectors to photon detectors, focal plane arrays, and single-photon avalanche detectors [1]. Nowadays you can reach any piece of information in a matter of milliseconds, or even less, due to the technological developments that have happened in the past several decades. The world is now full of different technologies that have made our lives much easier. It is so easy to communicate using many different means from landlines to optical fibers and satellite communications. The more communication methods develop, the more secure and fast transmission technology is needed. This fact forces the scientific community to develop light-transmitting systems and these needs support a big interest in the light detection area.

Currently, nanostructures with quantum wells (QW) and quantum dots (QD) are very widely used to create photodetectors in the visible and infrared ranges. At the same time, for various applications, various semiconductor material systems are used that most fully satisfy the specific requirements for device structures: III–V (GaAs, AlGaAs, etc.), II–VI (CdHgTe), IV–IV (GeSi, GeSn, GeSiSn), and others. However, all their potentialities are not implemented so far and they remain one of the most promising structures for creating optoelectronic devices.

A characteristic feature of all types of low-dimensional structures is the manifestation of the effects of spatial (dimensional) quantization, caused by the limitation of the free movement of charge carriers in one or several directions. Size quantization effects lead to a significant change in the energy spectrum of electrons and holes and the appearance of discrete energy levels and intermediate-allowed energy bands entirely located in the band gap of the semiconductor. This, in turn, leads to the appearance of new unique properties of such structures, which make it possible to create completely new types of optoelectronic devices on their basis [2].

For the first time, the existence of spatial quantization effects in low-dimensional semiconductor structures (nanostructures) was experimentally demonstrated by Dingle et al. in the first half of the 1970s when studying optical properties of AlGaAs-GaAs heterostructures with GaAs quantum well [3]. Germanium quantum dots in silicon became

one of the central themes of research in the early 1990s, when they were first obtained in the experiments by Eaglesham, Mo et al. [4,5]. Almost immediately, quantum-well effects were observed experimentally in this system [6].

The main requirements for choosing photodetectors are good performance, operation at the highest possible temperatures, and low manufacturing costs. In addition, today it seems necessary to create on a single chip the entire set of components of fiber-optic communication lines, including light-emitting devices and photodetectors. To reduce the costs of such systems, it is necessary that a larger number of components be made on the basis of typical silicon technology methods.

Silicon itself is transparent to radiation with a wavelength greater than 1.1 microns. Good photosensitivity in the region of $\lambda \approx 1.5$ μm is possessed by germanium photodetectors. The Ge/Si system may be also supplemented by tin, which extends the responsivity up to 2 μm. In this regard, prospects are outlined for the creation of high-speed photodetectors based on Si–Ge–Sn heterostructures with high sensitivity at room temperature in the spectral range of quartz fiber transparency of 1.3 and 1.55 μm.

Besides that, the adding of tin provides an opportunity to control the lattice constant and energy gap independently. Among the other advantages of group-IV materials is the possibility to create multispectral detectors, rather high mobility of carriers, and fast-speed operation, along with low noise, simple design, and highly-developed technology of synthesis.

The integration of silicon, germanium, and tin heterostructures with a silicon chip and their compatibility with silicon electronic and photonic circuits has great potential for the development of low-cost telecommunication optoelectronic modules for fiber optic communication lines operating in the telecommunication wavelength range [7–13].

One of the main methods for obtaining low-dimensional structures today is molecular beam epitaxy, the main advantages of which include low temperatures and growth rates, the possibility of abrupt interruption and resumption of growth, and precise control of the composition of the main substance and impurity concentrations. In this case, the analysis of the grown structures and the control of the necessary parameters can be carried out directly in the synthesis process.

Molecular beam epitaxy and other modern technological and material advances in semiconductors have brought the possibility of fabricating heterostructures utilizing quantum mechanical features. For example, creating quantum wells and self-assembled quantum dots allowed researchers to manufacture better photodetectors with higher performance.

In this review, we considered the latest and most modern photodetectors in the current scientific literature, stating the types and materials while highlighting the features of each work with special attention to Ge-Si photodetectors. These heterostructures with quantum wells and dots have a number of unique properties that made it striking to scientists' attention and device applications. Since silicon is the dominating semiconductor material in the electronic industry over the past decades, and as germanium nanostructures are very compatible with silicon, that made them a better fit and promising candidate to use in future technologies.

2. Thin Film and Quantum Well Photodetectors

A quantum well is a very thin layer of one material with narrow bandgap is situated between two materials with wider bandgaps. As a result a potential step is formed. This potential well limits the motion of carriers in one direction while they are free to move in two other directions. When the width of the potential well is small enough, the energy spectrum of carriers becomes discrete and their motion in the thin layer becomes quantized. In this review we will consider one of the simplest quantum well devices—quantum well photodetector.

The quantum well photodetector operation relies on the intersubband absorption within either the conduction band (for electrons) or the valence band (for holes). The principle of operation of a quantum well photodetector can be explained by the basic laws

of quantum mechanics. The quantum well is equivalent to the classical problem of motion of a particle in a box. To obtain the energy spectrum of such particle the time independent Schrödinger equation should be solved.

The SiGe/Si material system almost immediately proved to be perspective for various applications of nanostructures in electronics and optoelectronics. Then, SiGeSn material system in various combinations of constituent elements became very promising, since within their framework it is possible to control the band gap and obtain direct-gap semiconductors. These materials can be used to create photodetectors, solar cells, and light-emitting devices, successfully competing with materials traditionally for optoelectronics based on III–V and II–VI compounds [14–23].

GeSn techniques have drawn a lot of attention of Si-based technology in the last couple decades because the operating wavelengths range of this system spreads into the near infrared and short-wave infrared regions. Generally, scientific research on GeSn detectors has involved an increase in the past decade leading to the development of high-performance GeSn detectors. Today, there are several photodetectors based on Si-Ge. One of them is Ge-Si-Sn alloy, which is widely used in quantum well infrared photodetectors.

For example, in the work [24] a photoconductor detector made of one layer of GeSn on Ge, and working in the range between 1.5–2 μm, was shown (Figure 1).

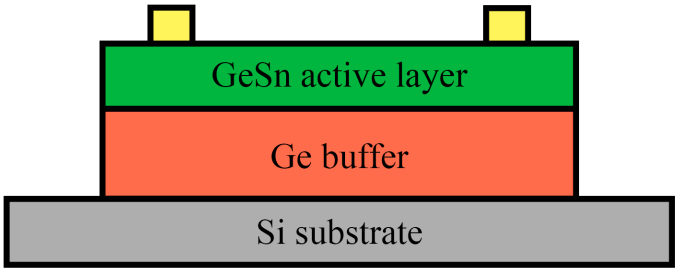

Figure 1. Cross-section view of the one-layer GeSn on Ge photoconductor.

The photoconductor GeSn samples used in this photodetector were grown using a reduced-pressure chemical vapor deposition technology. A study has been conducted on this photoconductor using 0.9, 3.2, and 7% Sn. Electrical and optical characteristics under 300 to 77 K were measured and the results of the detectivity, dark current, and responsivity were observed and measured under equivalent conditions. It was noted that the higher the temperature the less the performance of this photodetector is, which is caused by the decrease in the number of thermally activated carriers. This leads to a higher noise currents, while the responsivity of the photoconductor shows the linear increase with applied voltage that is indicative of the photoconductive gain [24].

Another study has been made on GeSn alloy where a photodiode with one layer of Ge quantum well was investigated [25]. The structure was grown on Si by molecular beam epitaxy. Figure 2 shows a schematic cross-section of the p-i-n photodetector structure. The photodetector was fabricated with quasiplanar technology.

The 1550 nm photodiode was investigated and the electrical and optical characteristics were measured under certain conditions. The dark current density of the photodiode increased by more than one order of magnitude, which was due to the high Sn concentration in this sample. The optical responsivity of the photodetector was also studied, which had shown the excellent quality of the fabricated GeSn layers.

A different study had been done based on one layer GeSn on Si [26]. The GeSn samples were grown using reduced-pressure chemical vapor deposition technologies and mesa structures were fabricated by photolithography and wet chemical etch processes. Figure 3 shows a schematic cross-sectional view of the photodetector.

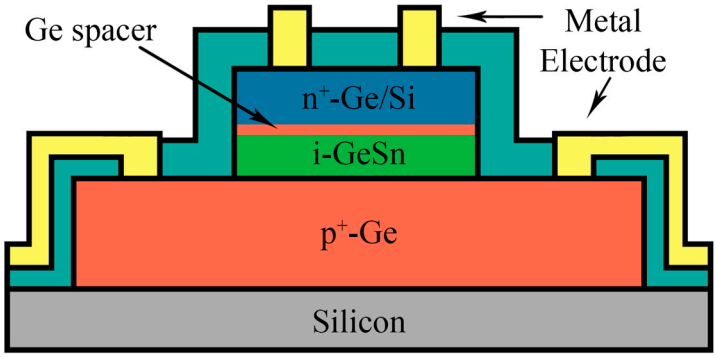

Figure 2. Schematic cross-section of the GeSn on Ge p-i-n photodiode structure.

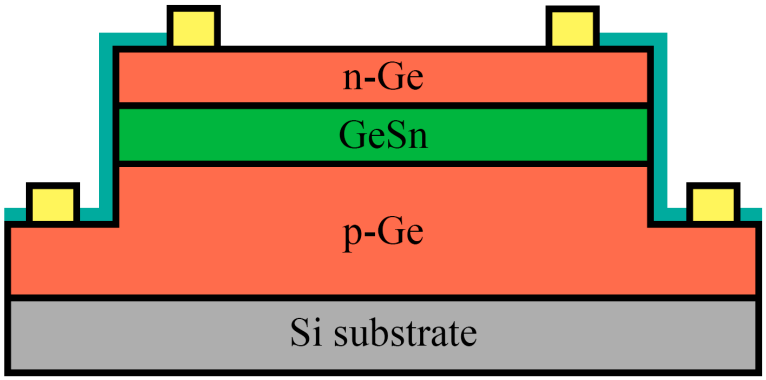

Figure 3. Schematic cross-sectional view of the GeSn on Ge p-i-n photodetector.

There were two samples with 7% and 10% tin. Electrical and optical characteristics were investigated for both samples. The reverse current density increased with the temperature as a result larger number of thermally activated carriers. The 10% Sn device showed higher current densities compared to that of the 7% Sn device at equal conditions due to the narrower bandgap, which also resulted in the larger number of thermally excited carriers. Other parameters were also studied such as detectivity for both samples. They have shown very close values under the same conditions [26]. This study has shown good performance and detectivity compared with the detectors dominating the market.

The next study with one layer structure used Ge on the Si system [27]. This paper considered a photodiode working at 1550 nm and consisting of a 300 nm thick Ge layer, which was fabricated using molecular beam epitaxy and standard etching and lithography techniques. The Ge p-i-n diode was grown on the Si substrate and covered by doped silicon capping layer. After the fabrication of p-i-n photodiode, the back side of the substrate was covered by black silicon. Optical power was induced from the rear side. The diameter of the mesa-structure was 400 μm, which is shown in Figure 4.

It was noted that the black silicon nanostructure did not spoil the I-V characteristics and acted similar to waveguide structures. This article established that the application of black silicon light-trapping structures is a possible technology to increase the responsivity of Ge-on-Si photodiodes. Besides that, rather good combination of bandwidth and responsivity was achieved, making these structures viable for ultra-fast applications for communication [27].

To enhance the absorption efficiency of the detector multiple layers with quantum wells may be used. One example with a GeSn/Ge multiple quantum wells (MQW) detector was shown in the recent work by Zhou et al. [28]. The multilayer p-i-n structure was grown on a 300-mm Ge-buffered Si substrate by reduced pressure chemical vapor deposition. Figure 5 shows a schematic diagram of the photodetector with a photon-trapping microstructure.

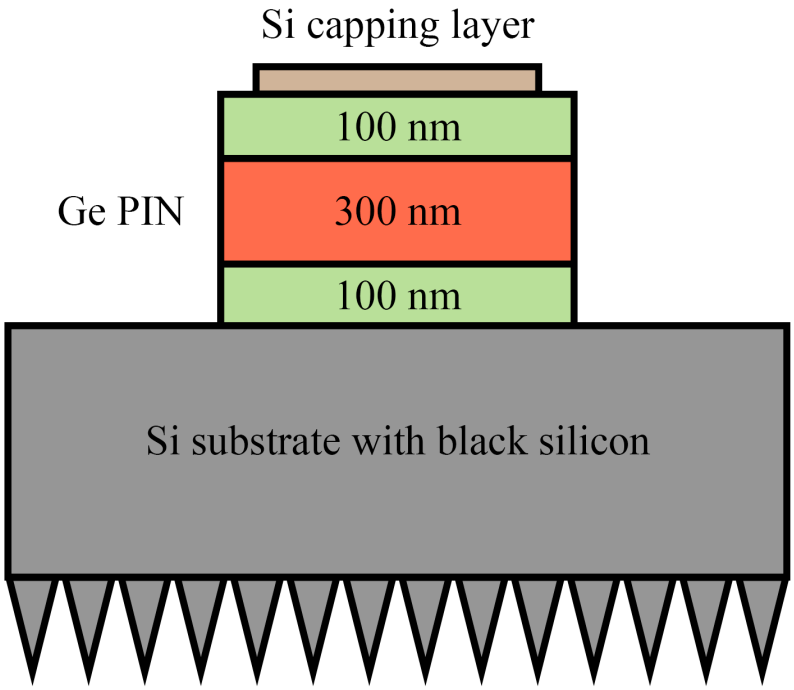

Figure 4. Scheme of the black silicon Ge-on-Si photodiode.

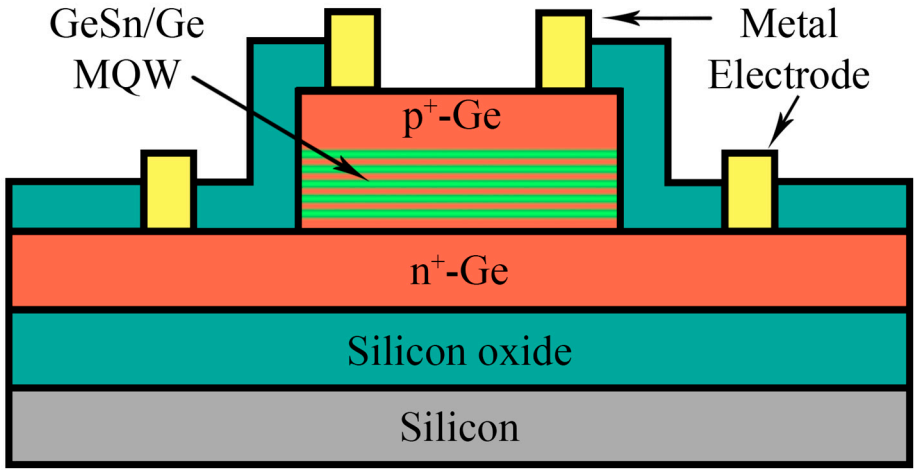

Figure 5. Schematic diagram of the multiple quantum wells GeSn/Ge photodetector with photon-trapping microstructure.

Characteristics investigations were made which have shown a flat photo response curve under a reverse bias voltage that indicates an efficient collection of photon-generated carriers and the capability of the photodetector regarding low-energy consumption. The dark current was investigated with and without a photon-trapping structure at room temperature. A low dark current density of 31.5 mA/cm^2 was achieved which is higher if compared with other photodetectors, and is also considered to be among the lowest for group-IV photodetectors. The dark current density increased to 45.2 mA/cm^2 at −1 V when the photon-trapping microstructure was incorporated. It was investigated and revealed that the increased dark current density mainly results from the increased surface leakage current introduced by the photon-trapping microstructure [28].

To sum up, these works enable group-IV photodetectors to be very perspective for various infrared systems. It is also desirable to monolithically integrate these detectors with lasers, transistors, waveguides, modulators and other devices on one silicon platform.

A lattice matched SiGeSn multiple quantum well structures should be developed to reduce the noise currents of this type of photodetectors in the future [28].

3. Quantum Dot Photodetectors

A quantum dot is a nanometer-sized semiconductor particle. The concept of "artificial atoms", or quantum dots, has emerged since the implement of molecular beam epitaxy and the first work on the reduced dimensionality of semiconductors. Quantum dots are widely used for their fully discrete energy spectrum and unique optical properties due to quantum size effects. They absorb and emit light of specific wavelengths if their energy spectra are matched. These wavelengths can be accurately controlled by changing size, shape or material composition of the particle. Hence, quantum dots are exploited in active layers for many widely-spread devices, for example, quantum dot displays and photon detectors.

Thus, an alternative to photodetectors based on quantum wells can be photodetectors with quantum dots. Such heterostructures are promising for photovoltaic applications and as receiving modules in fiber optic communication lines. Quantum dots have been successfully integrated in existing types of photodetectors, significantly enhancing their performance.

To realize all the potential advantages of photodetectors with quantum dots for the near-infrared range (increased sensitivity to normally incident radiation, high photoelectric multiplication factor, low thermal generation rate, narrow sensitivity range), the photosensitive region of the detector must contain an array of quantum dots with high density (on the order of 10^{11}–10^{12} cm^{-2}) [7,29–31].

The principles of operation of a photodetector with quantum dots are similar to those with quantum wells. The only difference is that in a quantum dot, the carrier is limited in its movement in all three directions, hence, zero-dimensional systems of carriers are realized [32]. It is expected that due to this limitation, quantum dot photodetectors can provide a better performance, namely higher operating temperatures (due to longer carrier lifetimes), low dark current, and high photoelectric gain [33], which ultimately translates into high sensitivity and detectability [34]. In addition, due to different selection rules for the absorption of light in photodetectors with quantum dots, it becomes possible to absorb incident radiation polarized along the normal to the layers of quantum dots.

In order to achieve this regime, self-assembled islands are embedded into layers of semiconductors with a larger energy gap and appropriate band discontinuities. Due to their properties, quantum dots are of high interest to modern technologies.

Silicon-based semiconductor materials with nanosized germanium inclusions have been actively studied since the early 1990s [4,5]. Such nanoheterostructures with self-organizing germanium quantum dots on silicon, grown by molecular beam epitaxy, exhibit a number of new nanoscale effects (associated with low-dimensional quantization effects), which are promising from the point of view of their application in optoelectronic devices [35–40].

Next, we will introduce some of the recent scientific studies that contained a quantum dot infrared photodetector with different silicon-related materials and a different number of quantum dot layers.

Starting with one layer of quantum dots, the following study shows an ultrathin layer photodetector with Ge quantum dots [41]. A 13 nm active layer of Ge quantum dots in SiO_2 matrix was fabricated on n-Ge substrate with (100) orientation. Quantum dots diameters varied from approximately 3 to 8 nm. The schematic diagram of the photodetector is shown in Figure 6.

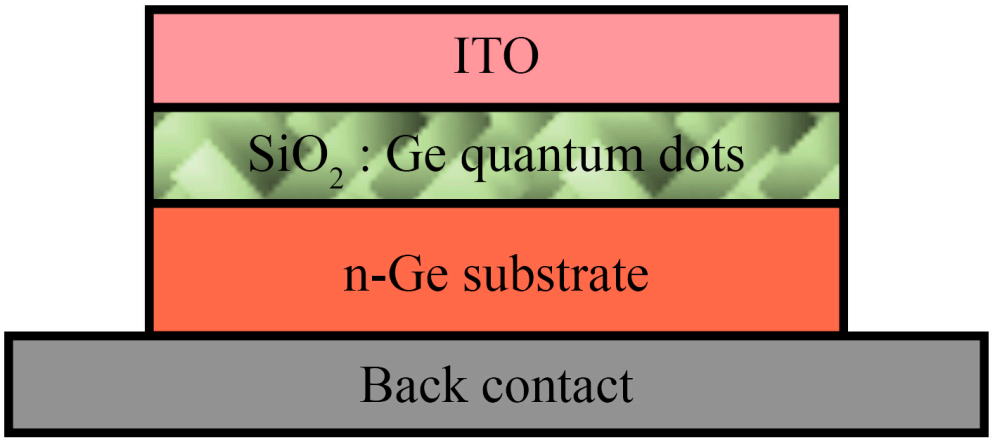

Figure 6. Schematic diagram of the photodetector consisting of an ITO electrode and an active layer with quantum dots on top of an n-Ge substrate.

The current-voltage characteristics of the photodetector were studied at various temperatures which varied from 77 K to 300 K in the dark and under illumination with the 640 and 1550 nm light. Reducing the active layer thickness to an ultrathin regime produced a high dark current at ambient conditions. Rise and fall times below 10 ns and 25 ns were achieved at −1 V in the visible and near-infrared ranges which is very promising [41]. This work has demonstrated that high quantum efficiency and fast response speed can be achieved in Ge quantum dot based photodetectors simultaneously at low voltage. Also, this work highlighted the importance of the thickness dependence of response speed in Ge quantum dot photodetectors.

A new example of quantum dot photodetectors was shown in the work [42]. Here a Ge quantum dot photodetector with one layer of quantum dots that has a thickness of 160 nm was fabricated. Ge and SiO_2 were cosputtered on the n-Ge substrate. The schematic diagram of the photodetector is shown in Figure 7.

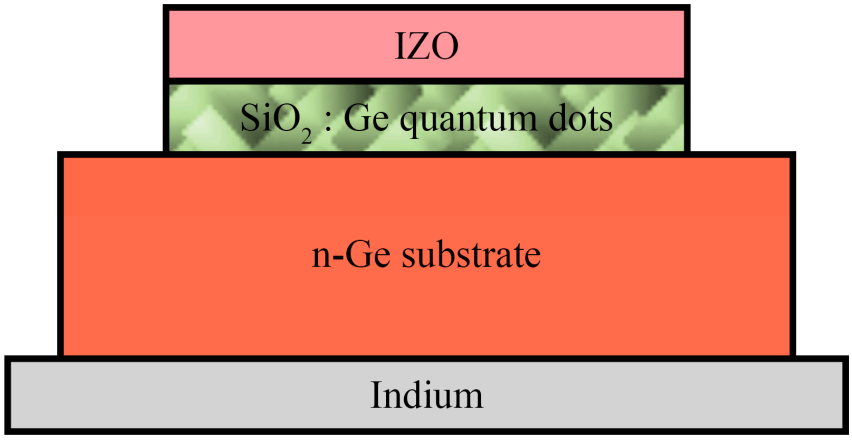

Figure 7. Schematic structure of the photodetector with Ge quantum dots in SiO_2.

The current-voltage characteristics were investigated in the range of wavelengths from 400 to 1550 nm. Results on the responsivity, reflectance, and quantum efficiency of the detector were presented and it was shown that the detector had its best performance and efficiency between 500–600 nm. High detectivity was achieved at the temperature range of 100–300 K [42].

Next, a midinfrared photodetector based on Ge quantum dots in Si has been presented [43]. The multilayer Si/Ge samples were synthesized by molecular beam epitaxy on the p^+-Si(001) substrate. The schematic design of the detector is shown in Figure 8.

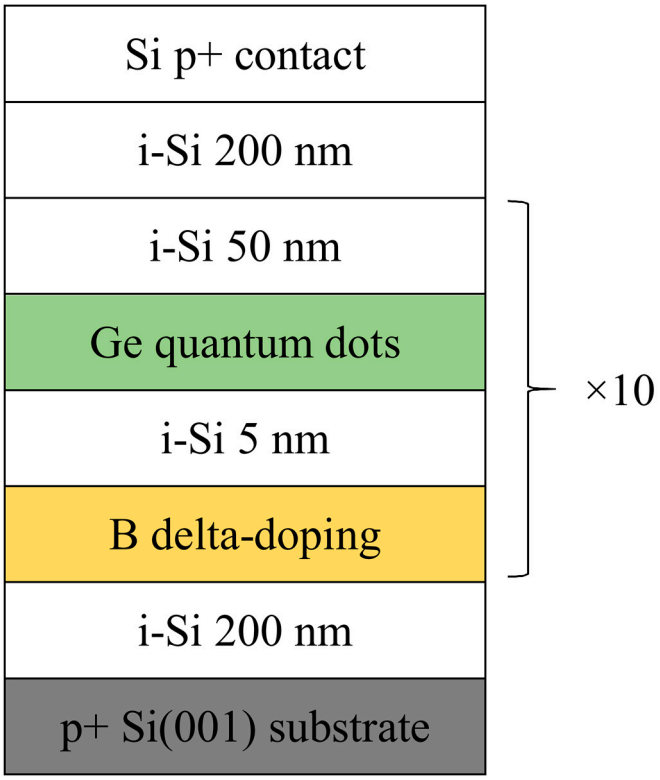

Figure 8. Schematic drawing of the Ge/Si photodetector with 10 layers of quantum dots.

Ten layers of germanium quantum dots separated by 50 nm silicon barriers served as active layers. Each Si barrier contained a boron delta-doping layer inserted 5 nm below the Ge-wetting layer. The active region was sandwiched between the 200-nm-thick intrinsic Si buffer and the cap layers. Finally, a 200-nm-thick p^+-Si top contact layer was deposited. The noise current, detectivity, and responsivity as a function of voltage and temperature were considered and the study has shown that such a device exhibited low dark current and operated until 200 K [43].

One more study with a multilayer quantum dot photodetector was introduced next where the multiple germanium quantum dot layers were grown on $Si_{0.82}Ge_{0.18}$ virtual substrate [44]. Ten layers of germanium quantum dots were separated by 35-nm $Si_{0.82}Ge_{0.18}$ barriers (Figure 9).

In this study another photodetector sample was fabricated based on pure silicon instead of SiGe for performance comparison purpose. Both samples have shown a responsivity in the whole mid-wave infrared range. Also, there was a significant improvement in the Ge/SiGe detector sensitivity over the wavelength region from 3 to 5 µm, as compared to the Ge/Si heterostructure. This is associated with the smaller hole effective mass in SiGe layers, which enables more efficient light absorption and photoexcited hole transportation. The photoconductive gain was studied and the noise characteristics were measured, and the SiGe detector has shown a larger gain, probably due to the increase of the hole mobility, and, therefore, the decrease of the hole transit time through the device. Moreover, in this work, a metallic plasmonic structure was added to the detector to achieve better performance of the quantum dot photodetector. The measured responsivity of the SiGe-based photodetector with and without the plasmonic structure have shown that plasmonic structures enhance photocurrent at the plasmon resonance frequencies compared with bare detectors [44].

The development of these works led to the emergence of the idea of using plasmonic effects and microresonators in order to enhance the properties of silicon-germanium photosensitive structures [45]. These attempts have shown a significant increase in the photodetector parameters, such as resonant responsivity, when using such plasmonic structures [46].

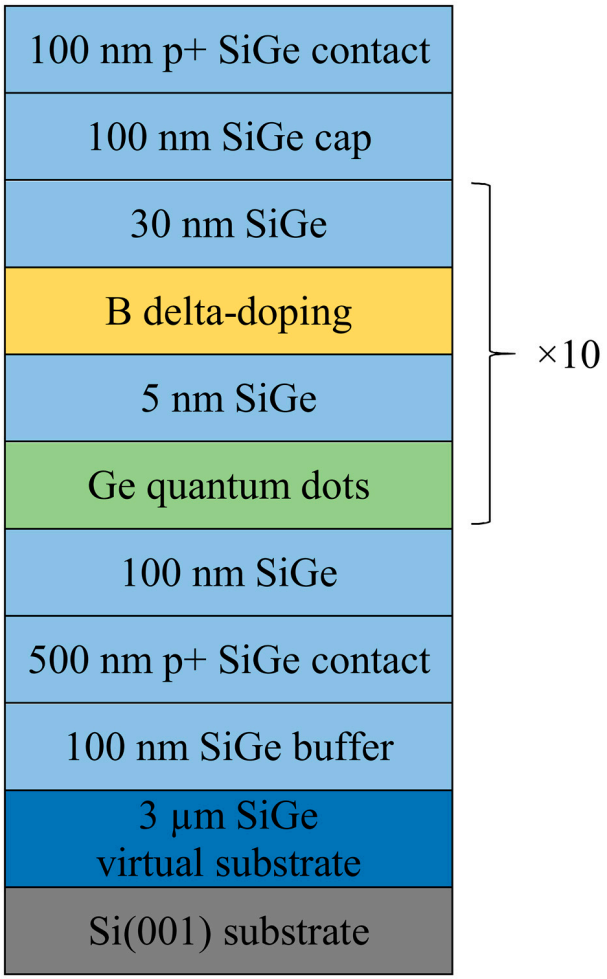

Figure 9. Schematic diagram of the Ge/SiGe photodetector with 10 layers of quantum dots.

Finally, we will discuss a study that has been made on a photodetector with mixed technologies for producing nanowires and quantum dots. Nanowires are structures where motion of carriers is limited in two of three directions.

In work [47], a silicon-on-insulator substrate was used for the growth of Ge quantum dots on silicon with subsequent fabrication of a quantum wire. Ge quantum dots were synthesized by molecular beam epitaxy. Quantum wires with the length of 10 μm and the width of 100 nm were fabricated by electron lithography. Figure 10 shows the cross-section of the fabricated photodetector.

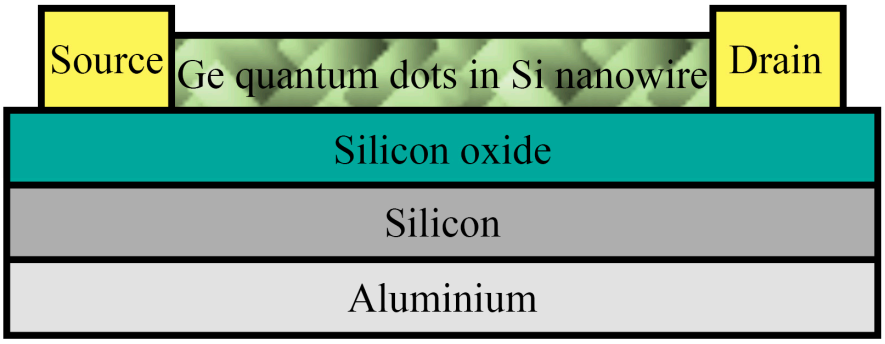

Figure 10. Schematic diagram of phototransistor with single Si nanowire decorated with Ge quantum dots.

This study demonstrated a simple and scalable fabrication process for achieving high-performance short-wave infrared photodetectors using Ge quantum dots in a single Si nanowire on CMOS-compatible SOI platforms. Moreover, the measurement of photocurrents with varying polarization of light revealed that the device can act as a polarization-sensitive photodetector [47].

4. Future Directions

Further development of the works on the fabrication of GeSn/Ge multiple-quantum-well p-i-n photodiodes has resulted in the simultaneous realization of low dark current and high detectivity in the structures similar to those shown in Figure 5. An ultralow dark current density of 16.3 mA/cm^2 was achieved in the work [48] due to the low threading dislocation density in the pseudomorphic GeSn layer [49], along with the high responsivity of 0.307 A/W and specific detectivity of 1.37×10^{10} cm·Hz$^{1/2}$·W^{-1} at 1550 nm. Even higher values of performance characteristics are theoretically predicted for the GeSn multiple quantum well photodetector with alternating layers of GeSn with different compositions [50]. The recently proposed approach suggests the use of a GeSn-on-insulator platform for the creation of metal-semiconductor-metal photodetectors with a sensitivity in the spectral range of up to 2.2 μm [51].

The works on using of GeSiSn solid solution layers have also confirmed that this material family is very promising for the fabrication of photodetectors in terms of extending their range of operating wavelengths and enhancing sensitivity [52–56].

The main problems of the application of nanostructures in photodetectors are connected with the low quality of the obtained structures. The improvement of technologies of synthesis should significantly increase the performance of quantum well and quantum dot photodetectors. The necessity to decrease the threading dislocation density, the number of different phase boundaries on the surface, and micro-cracks (caused by lattice mismatch) to suppress dark currents was stated repeatedly in the literature. On the other hand, tensile-strained layers may be used for the directed strain engineering of the energy spectra.

Where quantum dots are concerned, they have lower dark currents than quantum well structures due to their higher activation energy of thermionic emission (because of strong quantum confinement of carriers) and reduced phonon scattering, resulting in a longer carrier lifetime. However, it is very important to achieve the highest possible homogeneity of the ensemble of nanoislands in terms of their shape and size to reduce dark current densities. Special growth modes or prepattering of the surface for the creation of sites of preferable formation of nanoislands (selective growth) are used to improve the homogeneity. Another method of suppressing noise currents is the use of hybrid designs such as quantum dots in a quantum well and quantum dots in a quantum wire, which allows the researchers to achieve lower dark current densities and higher operating temperatures by proper control and optimization of the thickness of a well or nanowire.

The performance characteristics of the photodetectors reviewed in the previous sections are summarized in Table 1. It may be concluded that in terms of their performance photodetectors based on group-IV elements approach their III–V and II–VI competitors, showing values of detectivities of an order of 10^{12} cm·Hz$^{1/2}$·W^{-1} [57,58].

The use of various photon-trapping structures [59,60] and the creation of artificial roughness on one side of the detector is a typical route to increase the absorption coefficient and quantum efficiency of the device. For example, alternating materials with different refractive indices by heteroepitaxy results in a significant reflection at the interfaces. This is used to create optical Fabry-Perot resonators that reflect light back to the optical absorbing layer, thus effectively increasing the width of the physically thin absorbing layer. These techniques may also include exploiting distributed Bragg reflectors [61], capping the photosensitive structure with antireflection coatings [62], or using waveguide structures [63–71]. Works on the development of new designs of nanostructures [72,73], using graphene-like 2D materials [74–78] and exploiting the resonant cavity [79–81] and plasmonic effects [82,83] are also constantly being carried out.

Table 1. Comparison of the performance characteristics of various types of photodetectors.

Model	Wavelength	Responsivity	Dark Current Density	Detectivity
	nm	**A/W**	**mA/cm^2**	**cm·Hz$^{1/2}$·W^{-1}**
One layer GeSn/Ge photoconductor [24]	1550–2000	0.18	–	$1.0 \cdot 10^9$
One layer Ge/GeSn/Ge p-i-n photodiode [25]	1550	0.22	70	–
One layer Ge/GeSn/Ge photodetector [26]	1550–2600	0.30	10	$4.0 \cdot 10^9$
Black silicon Ge-on-Si p-i-n photodiode [27]	1550	0.34	150	–
Multiple quantum wells GeSn/Ge photodetector [28]	1550–2200	0.11	40	$2.1 \cdot 10^8$
Multiple quantum wells GeSn/Ge photodetector [48]	1550–2200	0.31	16	$1.4 \cdot 10^{10}$
One layer SiO_2: Ge QDs/Ge photodetector [41]	640–1550	0.47	–	–
One layer SiO_2: Ge QDs/Ge photodetector [42]	400–1550	1.12	–	$2.0 \cdot 10^{10}$
Multiple layer Ge QDs/Si photodetector [43]	up to 4000	0.43	10^{-6}	$6.2 \cdot 10^{10}$
Multiple layer Ge QDs/SiGe photodetector [44]	up to 6000	40	–	$1.4 \cdot 10^{11}$
Si nanowire: Ge QDs/SiO_2/Si phototransistor [47]	1200–1700	5.50	–	$9.3 \cdot 10^{11}$

One more complex way for the integration of photodetectors on a silicon chip is the fabrication of III–V epitaxial structures [84] or colloidal quantum dots [85–88] on a silicon substrate. Elements of other groups may also be used as a dopant in silicon or germanium [89,90]. Moreover, germanium photodiodes manufactured on Ge-on-insulator substrate, already showing very high performance, also fit the requirements of silicon-based technology [91]. Search for exotic nongroup IV elements combined with silicon is another route for the evolution of Si-compatible detectors [92].

In pace with the development of silicon-based photodetectors, a huge amount of work on the creation of group IV avalanche detectors (including single-photon avalanche diodes, SPAD) is carried out [93–95]. They are vital for a wide range of employment, from medical and LIDAR applications to quantum communication technologies [96–98]. Over the past decade, the academic and industrial community has achieved tremendous results in the improvement of the performance of SPADs [99–101].

Another very promising direction of further development in the field of silicon-based integration of electronic and photonic devices [102] is the creation of group IV light-emitting structures [103–105]. In recent years significant progress was achieved in the realization of GeSn [106–108] and diamond [109] laser-active media. The use of the GeSiSn ternary compound to improve the light-emitting characteristics of such structures also appears to be very promising [110]. Quantum dots are also considered important light-emitting nanostructures and have been intensively studied for several decades from the point of view of experimental aspects of the synthesis [111–120], their optical properties [121], and applications [122–125]. Finally, efficient group-IV single photon sources and semiconductor qubits [126–130] were recently shown, supporting the development of on-chip quantum information processing.

5. Conclusions

The performance of various types of photodetectors based on silicon, germanium, and tin is rapidly improving due to the dedicated efforts of many research groups. The bandwidth and quantum efficiency of such devices are comparable to those of their competitors in the face of devices based on III–V compounds and are sufficient for a number of applications. Thus, at present, no serious barriers are foreseen for the widespread use of Si-compatible group-IV-based nanostructured photodetectors.

The main advantages of silicon-based electronics and photonics, including their relative cheapness, highly-developed technology of synthesis, compatibility with silicon integrated circuits and CMOS-compatibility, opportunity to create multi-spectral detectors, and many others, make the research and industrial community confident in the long and bright future of this material system.

The reviewed devices may play a pivotal role in the establishment of anticipated low-cost and high-performance Si-based photonic-integrated circuits. All these results allow us to count on solving the problem of integrating all optoelectronic components on a single silicon chip in the nearest future.

Author Contributions: Conceptualization, K.L., A.K.; writing—original draft preparation, R.D., K.L., H.D., V.D. and K.K.; writing—review and editing, K.L.; supervision, A.K.; project administration A.K.; funding acquisition, A.K. All authors have read and agreed to the published version of the manuscript.

Funding: This research was funded by the Ministry of Science and Higher Education of the Russian Federation, grant number FSWM-2020-0048.

Institutional Review Board Statement: Not applicable.

Informed Consent Statement: Not applicable.

Data Availability Statement: The authors declare that the data supporting the findings of this study are available within the article.

Acknowledgments: The reported study was supported by the Tomsk State University Development Programme (Priority 2030, No. 2.0.6.22).

Conflicts of Interest: The authors declare no conflict of interest.

References

1. Rogalski, A. *Infrared Detectors*; CRC Press: Boca Raton, FL, USA, 2011; 876p.
2. Lozovoy, K.A.; Voitsekhovskiy, A.V.; Kokhanenko, A.P.; Satdarov, V.G.; Pchelyakov, O.P.; Nikiforov, A.I. Heterostructures with self-organized quantum dots of Ge on Si for optoelectronic devices. *Opto-Electron. Rev.* **2014**, *22*, 171–177. [CrossRef]
3. Dingle, R.; Wiegmann, W.; Henry, C.H. Quantum states of confined carriers in very thin $Al_xGa_{1-x}As$-GaAs-$Al_xGa_{1-x}As$ heterostructures. *Phys. Rev. Lett.* **1974**, *33*, 827–830. [CrossRef]
4. Eaglesham, D.J.; Cerullo, M. Dislocation-free Stranski–Krastanov growth of Ge on Si(100). *Phys. Rev. Lett.* **1990**, *64*, 1943–1946. [CrossRef] [PubMed]
5. Mo, Y.-W.; Savage, D.E.; Swartzentruber, B.S.; Lagally, M.G. Kinetic pathway in Stranski–Krastanov growth of Ge on Si(001). *Phys. Rev. Lett.* **1990**, *65*, 1020–1023. [CrossRef]
6. Yakimov, A.I.; Markov, V.A.; Dvurechenskii, A.V.; Pchelyakov, O.P. 'Coulomb staircase' in Si/Ge structure. *Philos. Mag. B* **1992**, *65*, 701–705. [CrossRef]
7. Pchelyakov, O.P.; Dvurechensky, A.V.; Latyshev, A.V.; Aseev, A.L. Ge/Si heterostructures with coherent Ge quantum dots in silicon for applications in nanoelectronics. *Semicond. Sci. Technol.* **2011**, *26*, 014027. [CrossRef]
8. Wei, R.; Deng, N.; Dong, H.; Ren, M.; Zhang, L.; Chen, P.; Liu, L. Ge quantum-dot polysilicon emitter heterojunction phototransistors for 1.31–1.55 μm light detection. *Mater. Sci. Eng. B* **2008**, *147*, 187–190. [CrossRef]
9. Elcurdi, M.; Boucaud, P.; Sauvage, S. Near-infrared waveguide photodetector with Ge/Si self-assembled quantum dots. *Appl. Phys. Lett.* **2002**, *80*, 509–511. [CrossRef]
10. Tong, S.; Liu, J.L.; Wan, J.; Wang, K.L. Normal-incidence Ge quantum-dot photodetectors at 1.5 μm based on Si substrate. *Appl. Phys. Lett.* **2002**, *80*, 1189–1191. [CrossRef]
11. Masini, G.; Colace, L.; Assanto, G. 2.5 Gbit/s polycrystalline germanium-on-silicon photodetector operating from 1.3 to 1.55 μm. *Appl. Phys. Lett.* **2003**, *82*, 2524–2526. [CrossRef]
12. Elving, A.; Hansson, G.V.; Ni, W.-X. SiGe (Ge-dot) heterojunction phototransistor for efficient light detection at 1.3–1.55 μm. *Physica E Low-Dimens. Syst. Nanostruct.* **2003**, *16*, 528–532. [CrossRef]

13. Yu, J.; Kasper, E.; Oehme, M. 1.55 μm resonant cavity enhanced photodiode based on MBE grown Ge quantum dots. *Thin Solid Film.* **2006**, *508*, 396–398. [CrossRef]
14. Jenkins, D.W.; Dow, J.D. Electronic properties of metastable Ge_xSn_{1-x} alloys. *Phys. Rev. B* **1987**, *36*, 7994–8000. [CrossRef] [PubMed]
15. Bauer, M.; Taraci, J.; Tolle, J.; Chizmeshya AV, G.; Zollner, S.; Smith, D.J.; Menendez, J.; Hu, C.; Kouvetakis, J. Ge-Sn semiconductors for band-gap lattice engineering. *Appl. Phys. Lett.* **2002**, *81*, 2992–2994. [CrossRef]
16. Ferry, D.K.; Bird, J.P.; Akis, R. Quantum dots: Applications in technology and in quantum physics. *Physica E Low-Dimens. Syst. Nanostruct.* **2004**, *25*, 298–302. [CrossRef]
17. Paul, D.J. Si/SiGe heterostructures: From material and physics to devices and circuits. *Semicond. Sci. Technol.* **2004**, *19*, 75–108. [CrossRef]
18. Wang, K.L.; Tong, S.; Kim, H.J. Properties and applications of SiGe nanodots. *Mater. Sci. Semicond. Process.* **2005**, *8*, 389–399. [CrossRef]
19. Kouvetakis, J.; Chizmeshya AV, G. New classes of Si-based photonic materials and device architectures via designer molecular routes. *J. Mater. Chem.* **2007**, *17*, 1649–1655. [CrossRef]
20. Roucka, R.; Xie, J.; Kouvetakis, J.; Mathews, J.; D'Costa, V.; Menendez, J.; Tolle, J.; Yu, S.-Q. $Ge_{1-y}Sn_y$ photoconductor structures at 1.55 μm: From advanced materials to prototype devices. *J. Vac. Sci. Technol. B* **2008**, *26*, 1952–1959. [CrossRef]
21. D'Costa, V.R.; Fang, Y.-Y.; Tolle, J.; Kouvetakis, J.; Menendez, J. Tunable Optical Gap at a Fixed Lattice Constant in Group-IV Semiconductor Alloys. *Phys. Rev. Lett.* **2009**, *102*, 107403. [CrossRef]
22. D'Costa, V.R.; Fang, Y.-Y.; Tolle, J.; Kouvetakis, J.; Menendez, J. Ternary GeSiSn alloys: New opportunities for strain and band gap engineering using group-IV semiconductors. *Thin Solid Film.* **2010**, *518*, 2531–2537. [CrossRef]
23. Wu, J.; Chen, S.; Seeds, A.; Liu, H. Quantum dot optoelectronic devices: Lasers, photodetectors and solar cells. *J. Phys. D Appl. Phys.* **2015**, *48*, 363001. [CrossRef]
24. Conley, B.R.; Mosleh, A.; Ghetmiri, S.A.; Du, W.; Soref, R.A.; Sun, G.; Margetis, J.; Tolle, J.; Naseem, H.A.; Yu, S.Q. Temperature dependent spectral response and detectivity of GeSn photoconductors on silicon for short wave infrared detection. *Opt. Express* **2014**, *22*, 15639–15652. [CrossRef] [PubMed]
25. Oehme, M.; Kostecki, K.; Ye, K.; Bechler, S.; Ulbricht, K.; Schmid, M.; Kaschel, M.; Gollhofer, M.; Körner, R.; Zhang, W.; et al. GeSn-on-Si normal incidence photodetectors with bandwidths more than 40 GHz. *Opt. Express* **2014**, *22*, 839–846. [CrossRef]
26. Pham, T.; Du, W.; Tran, H.; Margetis, J.; Tolle, J.; Sun, G.; Soref, R.A.; Naseem, H.A.; Li, B.; Yu, S.Q. Systematic study of Si-based GeSn photodiodes with 2.6 μm detector cutoff for short-wave infrared detection. *Opt. Express* **2016**, *24*, 4519–4531. [CrossRef]
27. Steglich, M.; Oehme, M.; Kasebier, T.; Zilk, M. Ge-on-Si photodiode with black silicon boosted responsivity. *Appl. Phys. Lett.* **2015**, *107*, 051103. [CrossRef]
28. Zhou, H.; Xu, S.; Lin, Y.; Huang, Y.C.; Son, B.; Chen, Q.; Guo, X.; Lee, K.H.; Goh, S.C.K.; Gong, X.; et al. High-efficiency GeSn/Ge multiple-quantum-well photodetectors with photon-trapping microstructures operating at 2 μm. *Opt. Express* **2020**, *28*, 10280–10293. [CrossRef] [PubMed]
29. Yakimov, A.I.; Dvurechenskii, A.V.; Nikiforov, A.I. Germanium Self-Assembled Quantum Dots in Silicon for Nano- and Optoelectronics. *J. Nanoelectron. Optoelectron.* **2006**, *1*, 119–175. [CrossRef]
30. Martyniuk, P.; Rogalski, A. Quantum-dot infrared photodetectors: Status and outlook. *Prog. Quantum Electron.* **2008**, *32*, 89–120. [CrossRef]
31. Barve, A.V.; Lee, S.J.; Noh, S.K.; Krishna, S. Review of current progress in quantum dot infrared photodetectors. *Laser Photonics Rev.* **2010**, *4*, 738–750. [CrossRef]
32. Yakimov, A.I.; Kirienko, V.V.; Armbrister, V.A.; Bloshkin, A.A.; Dvurechenskii, A.V. Phonon bottleneck in p-type Ge/Si quantum dots. *Appl. Phys. Lett.* **2015**, *107*, 213502. [CrossRef]
33. Liu, G.; Zhang, J.; Wang, L. Dark current model and characteristics of quantum dot infrared photodetectors. *Infrared Phys. Technol.* **2015**, *73*, 36–40. [CrossRef]
34. Mahmoodi, A.; Jahromi, H.D.; Sheikhi, M.H. Dark current modeling and noise analysis in quantum dot infrared photodetectors. *IEEE Sens. J.* **2015**, *15*, 5504–5509. [CrossRef]
35. Wang, K.L.; Cha, D.; Liu, J.; Chen, C. Ge/Si self-assembled quantum dots and their optoelectronic device applications. *Proc. IEEE* **2007**, *95*, 1866–1882. [CrossRef]
36. Aqua, J.-N.; Berbezier, I.; Favre, L. Growth and self-organization of SiGe nanostructures. *Phys. Rep.* **2013**, *522*, 59–189. [CrossRef]
37. Izhnin, I.; Fitsych, O.I.; Voitsekhovskii, A.V.; Kokhanenko, A.P.; Lozovoy, K.A.; Dirko, V.V. Nanostructures with Ge–Si quantum dots for infrared photodetectors. *Opto-Electron. Rev.* **2018**, *26*, 195–200. [CrossRef]
38. Brunner, K. Si/Ge nanostructures. *Rep. Prog. Phys.* **2002**, *65*, 27–72. [CrossRef]
39. Pchelyakov, O.P.; Bolkhovityanov Yu, B.; Dvurechenskii, A.V.; Nikiforov, A.I.; Yakimov, A.I.; Voigtlander, B. Molecular beam epitaxy of silicon-germanium nanostructures. *Thin Solid Film.* **2000**, *367*, 75–84. [CrossRef]
40. Krasilnik, Z.F.; Novikov, A.V.; Lobanov, D.N.; Kudryavtsev, K.E.; Antonov, A.V.; Obolenskiy, S.V.; Zakharov, N.D.; Werner, P. SiGe nanostructures with self-assembled islands for Si-based optoelectronics. *Semicond. Sci. Technol.* **2011**, *26*, 014029. [CrossRef]
41. Shi, S.; Pacifici, D.; Zaslavsky, A. Fast and efficient germanium quantum dot photodetector with an ultrathin active layer. *Appl. Phys. Lett.* **2021**, *119*, 221108. [CrossRef]
42. Siontas, S.; Wang, H.; Li, D.; Zaslavsky, A.; Pacifici, D. Broadband visible-to-telecom wavelength germanium quantum dot photodetectors. *Appl. Phys. Lett.* **2018**, *113*, 181101. [CrossRef]

43. Yakimov, A.I.; Bloshkin, A.A.; Timofeev, V.A.; Nikiforov, A.I.; Dvurechenskii, A.V. Effect of overgrowth temperature on the mid-infrared response of Ge/Si(001) quantum dots. *Appl. Phys. Lett.* **2012**, *100*, 053507. [CrossRef]
44. Yakimov, A.I.; Kirienko, V.V.; Bloshkin, A.A.; Armbrister, V.A.; Dvurechenskii, A.V.; Hartmann, J.M. Photovoltaic Ge/SiGe quantum dot mid-infrared photodetector enhanced by surface plasmons. *Opt. Express* **2017**, *25*, 25602–25611. [CrossRef] [PubMed]
45. Dvurechenskii, A.; Yakimov, A.; Kirienko, V.; Bloshkin, A.; Zinovyev, V.; Zinovieva, A.; Mudryi, A. Enhanced Optical Properties of Silicon Based Quantum Dot Heterostructures. *Defect Diffus. Forum* **2018**, *386*, 68–74. [CrossRef]
46. Yakimov, A.I.; Kirienko, V.V.; Bloshkin, A.A.; Dvurechenskii, A.V.; Utkin, D.E. Near-infrared photoresponse in Ge/Si quantum dots enhanced by localized surface plasmons supported by aluminum nanodisks. *J. Appl. Phys.* **2020**, *128*, 143101. [CrossRef]
47. John, J.W.; Dhyani, V.; Singh, S.; Jakhar, A.; Sarkar, A.; Das, S.; Ray, S.K. Low-noise, high-detectivity, polarization sensitive, room-temperature infrared photodetectors based on Ge quantum dot decorated Si-on-insulator nanowire field effect transistors. *Nanotechnology* **2021**, *32*, 315205. [CrossRef]
48. Zhou, H.; Xu, S.; Wu, S.; Huang, Y.-C.; Zhao, P.; Tong, J.; Son, B.; Guo, X.; Zhang, D.; Gong, X.; et al. Photo detection and modulation from 1,550 to 2,000 nm realized by a GeSn/Ge multiple-quantum-well photodiode on a 300-mm Si substrate. *Opt. Express* **2020**, *28*, 34772–34786. [CrossRef]
49. Li, X.; Peng, L.; Liu, Z.; Zhou, Z.; Zheng, J.; Xue, C.; Zuo, Y.; Chen, B.; Cheng, B. 30 GHz GeSn photodetector on SOI substrate for 2 μm wavelength application. *Photonics Res.* **2021**, *9*, 494–500. [CrossRef]
50. Kumar, H.; Pandey, A.K. GeSn-Based Multiple-Quantum-Well Photodetectors for Mid-Infrared Sensing Applications. *IEEE Trans. Nanobiosci.* **2022**, *21*, 175–183. [CrossRef]
51. Son, B.; Lin, Y.; Lee, K.H.; Margetis, J.; Kohen, D.; Tolle, J.; Tan, C.S. Metal-Semiconductor-Metal Photodetectors on a GeSn-on-Insulator Platform for 2 μm Applications. *IEEE Photonics J.* **2022**, *14*, 6824406. [CrossRef]
52. Timofeev, V.A.; Nikiforov, A.I.; Tuktamyshev, A.R.; Mashanov, V.I.; Loshkarev, I.D.; Bloshkin, A.A.; Gutakovskii, A.K. Pseudomorphic GeSiSn, SiSn and Ge layers in strained heterostructures. *Nanotechnology* **2018**, *29*, 154002. [CrossRef] [PubMed]
53. Timofeev, V.; Nikiforov, A.; Yakimov, A.; Mashanov, V.; Loshkarev, I.; Bloshkin, A.; Kirienko, V.; Novikov, V.; Kareva, K. Studying the morphology, structure and band diagram of thin GeSiSn films and their mid-infrared photoresponse. *Semicond. Sci. Technol.* **2019**, *34*, 014001. [CrossRef]
54. Sun, G.; Soref, R.A.; Khurgin, J.B.; Yu, S.-Q.; Chang, G.-E. Longwave IR lattice matched L-valley Ge/GeSiSn waveguide quantum cascade detector. *Opt. Express* **2022**, *30*, 42385–42393. [CrossRef]
55. Timofeev, A.A.; Mashanov, V.I.; Nikiforov, A.I.; Loshkarev, A.D.; Gulyaev, D.V.; Volodin, V.A.; Kozhukhov, A.S.; Komkov, O.S.; Firsov, D.D.; Korolkov, I.V. Study of structural and optical properties of a dual-band material based on tin oxides and GeSiSn compounds. *Appl. Surf. Sci.* **2022**, *573*, 151615. [CrossRef]
56. Timofeev, V.A.; Mashanov, V.I.; Nikiforov, A.I.; Skvortsov, I.V.; Gayduk, A.E.; Bloshkin, A.A.; Loshkarev, I.D.; Kirienko, V.V.; Kolyada, D.V.; Firsov, D.D.; et al. Tuning the structural and optical properties of GeSiSn/Si multiple quantum wells and GeSn nanostructures using annealing and a faceted surface as a substrate. *Appl. Surf. Sci.* **2022**, *593*, 153421. [CrossRef]
57. Siontas, S.; Li, D.; Wang, H.; Aravind AV, P.S.; Zaslavsky, A.; Pacifici, D. High-performance germanium quantum dot photodetectors in the visible and near infrared. *Mater. Sci. Semicond. Process.* **2019**, *92*, 19–27. [CrossRef]
58. Xu, G.; Cong, H.; Wan, F.; Wang, X.; Xie, C.; Xu, C.; Xue, C. Si-Based Ge 320 × 256 Focal Plane Array for Short-Wave Infrared Imaging. *IEEE Photonics Technol. Lett.* **2022**, *34*, 517–520. [CrossRef]
59. Gao, Y.; Cansizoglu, H.; Polat, K.G.; Ghandiparsi, S.; Kaya, A.; Mamtaz, H.H.; Mayet, A.S.; Wang, Y.; Zhang, X.; Yamada, T. Photon-trapping microstructures enable high-speed high-efficiency silicon photodiodes. *Nat. Photonics* **2017**, *11*, 301–308. [CrossRef]
60. Cansizoglu, H.; Bartolo-Perez, C.; Gao, Y.; Devine, E.P.; Ghandiparsi, S.; Polat, K.G.; Mamtaz, H.H.; Yamada, T.; Elrefaie, A.F.; Wang, S.-Y. Surface-illuminated photon-trapping high-speed Ge-on-Si photodiodes with improved efficiency up to 1700 nm. *Photonics Res.* **2018**, *6*, 734–742. [CrossRef]
61. Kumar, H.; Pandey, A.K.; Lin, C.-H. Optimal design and noise analysis of high-performance DBR-integrated lateral germanium (Ge) photodetectors for SWIR applications. *J. Electron Devices Soc.* **2022**, *10*, 649–659. [CrossRef]
62. Wu, S.; Xu, S.; Zhou, H.; Jin, Y.; Chen, Q.; Huang, Y.-C.; Zhang, L.; Gong, X.; Tan, C.S. High-Performance Back-Illuminated $Ge_{0.92}Sn_{0.08}$/Ge Multiple-Quantum-Well Photodetector on Si Platform for SWIR Detection. *IEEE J. Sel. Top. Quantum Electron.* **2022**, *28*, 8200109. [CrossRef]
63. Seo, D.; Kwon, W.-B.; Kim, S.C.; Park, C.-S. Frequency Response Estimation of 1.3 μm Waveguide Integrated Vertical PIN Type Ge-on-Si Photodetector Based on the Analysis of Fringing Field in Intrinsic Region. *Curr. Opt. Photonics* **2019**, *3*, 510–515.
64. Hu, X.; Wu, D.; Chen, D.; Wang, L.; Xiao, X.; Yu, S. 180 Gbit/s Si_3N_4-waveguide coupled germanium photodetector with improved quantum efficiency. *Opt. Lett.* **2021**, *46*, 6019–6022. [CrossRef]
65. Wang, H.; Zhang, J.; Zhang, G.; Chen, Y.; Huang, Y.-C.; Gong, X. High-speed and high-responsivity p-i-n waveguide photodetector at a 2 μm wavelength with a $Ge_{0.92}Sn_{0.08}$/Ge multiple-quantum-well active layer. *Opt. Lett.* **2021**, *46*, 2099–2102. [CrossRef] [PubMed]
66. Cui, J.; Chen, H.; Zhou, J.; Li, T. High Performance Ge-on-Si Photodetector With Optimized Light Field Distribution by Dual-Injection. *IEEE Photonics J.* **2022**, *14*, 6817304. [CrossRef]
67. Fu, Z.; Yu, H.; Wei, Z.; Xia, P.; Zhang, Q.; Wang, X.; Huang, Q.; Wang, Y.; Yang, J. High-Power and High-Speed Ge/Si Traveling-Wave Photodetector Optimized by Genetic Algorithm. *J. Light. Technol.* **2022**, *41*, 240–248. [CrossRef]

68. Wang, H.; Chen, Y.; Zhang, G.; Zhang, J.; Xu, H.; Huang, Y.-C.; Gong, X. Monolithic Waveguide-Integrated Group IV Multiple-Quantum-Well Photodetectors on 300 mm Si Substrates. *IEEE Trans. Electron Devices* **2022**, *69*, 2166–2172. [CrossRef]
69. Wang, H.; Zhang, J.; Zhang, G.; Chen, Y.; Han, K.; Huang, Y.-C.; Gong, X. Monolithic Waveguide Group IV Multiple-Quantum-Well Photodetectors and Modulators on 300-mm Si Substrates for 2-µm Wavelength Optoelectronic Integrated Circuit. *IEEE Trans. Electron Devices* **2022**, *69*, 7161–7166. [CrossRef]
70. Wei, Z.; Yu, H.; Fu, Z.; Xia, P.; Zhang, Q.; Ning, N.; Huang, Q.; Wang, Y.; Yang, J. Silicon-based high-power traveling wave photodetector with inductive gain peaking. *Opt. Express* **2022**, *30*, 46094–46105. [CrossRef]
71. Sia JX, B.; Li, X.; Wang, J.; Wang, W.; Qiao, Z.; Guo, X.; Lee, C.W.; Sasidharan, A.; Gunasagar, S.; Littlejohns, C.G.; et al. Wafer-Scale Demonstration of Low-Loss (~0.43 dB/cm), High-Bandwidth (>38 GHz), Silicon Photonics Platform Operating at the C-Band. *IEEE Photonics J.* **2022**, *14*, 6628609.
72. Li, Y.; Liu, X.; Li, X.; Wang, S.; Ye, H.; Zhang, L.; Li, Y.; Sun, S.; Chen, B.; Ma, Y.; et al. Surface illuminated interdigitated Ge-on-Si photodetector with high responsivity. *Opt. Express* **2021**, *29*, 16346–16361. [CrossRef] [PubMed]
73. Kumari, K.; Kumar, S.; Mehta, M.; Chatterjee, A.; Selvaraja, S.K.; Avasthi, S. Laser-Crystallized Epitaxial Germanium on Silicon-Based Near-Infrared Photodetector. *IEEE Sens. J.* **2022**, *22*, 11682–11689. [CrossRef]
74. Izhnin, I.I.; Kurbanov, K.R.; Lozovoy, K.A.; Kokhanenko, A.P.; Dirko, V.V.; Voitsekhovskii, A.V. Epitaxial fabrication of 2D materials of group IV elements. *Appl. Nanosci.* **2020**, *10*, 4375–4383. [CrossRef]
75. Dushaq, G.; Paredes, B.; Villegas, J.E.; Tamalampudi, S.R.; Rasras, M. On-chip integration of 2D Van der Waals germanium phosphide (GeP) for active silicon photonics devices. *Opt. Express* **2022**, *30*, 15986–15997. [CrossRef] [PubMed]
76. Lozovoy, K.A.; Dirko, V.V.; Vinarskiy, V.P.; Kokhanenko, A.P.; Voitsekhovskii, A.V.; Akimenko, N.Y. Two-dimensional materials of group IVA: Latest advances in epitaxial methods of growth. *Russ. Phys. J.* **2022**, *64*, 1583–1591. [CrossRef]
77. Guskov, A.; Lavrov, S.; Galiev, R. Polarization sensitive photodetectors based on two-dimensional WSe_2. *Nanomaterials* **2022**, *12*, 1854. [CrossRef]
78. Lozovoy, K.A.; Izhnin, I.I.; Kokhanenko, A.P.; Dirko, V.V.; Vinarskiy, V.P.; Voitsekhovskii, A.V.; Fitsych, O.I.; Akimenko, N.Y. Single-element 2D materials beyond graphene: Methods of epitaxial synthesis. *Nanomaterials* **2022**, *12*, 2221. [CrossRef]
79. Novikov, A.; Smagina, Z.; Stepikhova, M.; Zinovyev, V.; Rudin, S.; Dyakov, S.; Rodyakina, E.; Nenashav, A.; Sergeev, S.; Peretokin, A.; et al. One-stage formation of two-dimensional photonic crystal and spatially ordered arrays of self-assembled Ge(Si) nanoislands on pit-patterned silicon-on-insulator substrate. *Nanomaterials* **2021**, *11*, 909. [CrossRef]
80. Tsai, C.H.; Huang, B.J.; Soref, R.A.; Sun, G.; Cheng, H.H.; Chang, G. GeSn resonant-cavity-enhanced photodetectors for efficient photodetection at the 2 µm wavelength band. *Opt. Lett.* **2020**, *45*, 1463–1466. [CrossRef]
81. Berkmann, F.; Augel, L.; Hack, M.; Kawaguchi, Y.; Weisshaupt, D.; Fischer, I.A.; Schulze, J. Optimization of Fully Integrated Al Nanohole Array-Based Refractive Index Sensors for Use With a LED Light Source. *IEEE Photonics J.* **2022**, *14*, 4831708. [CrossRef]
82. Srikam, S.; Traiwattanapong, W.; Limsuwan, P.; Chaisakul, P. An FDTD Investigation of Compact and Low-Voltage Waveguide-Integrated Plasmonic Ge/SiGe Multiple Quantum Wells Photodetectors. *IEEE Photonics J.* **2022**, *14*, 6650207. [CrossRef]
83. Zhou, H.; Zhang, L.; Tong, J.; Wu, S.; Son, B.; Chen, Q.; Zhang, D.H.; Tan, C.S. Surface plasmon enhanced GeSn photodetectors operating at 2 µm. *Opt. Express* **2021**, *29*, 8498–8509. [CrossRef] [PubMed]
84. Huang, J.; Guo, D.; Deng, Z.; Chen, W.; Liu, H.; Wu, J.; Chen, B. Midwave Infrared Quantum Dot Quantum Cascade Photodetector Monolithically Grown on Silicon Substrate. *J. Light. Technol.* **2018**, *36*, 4033–4038. [CrossRef]
85. Masala, S.; Adinolfi, V.; Sun, J.-P.; Del Gobbo, S.; Voznyy, O.; Kramer, I.J.; Hill, I.G.; Sargent, E.H. The silicon:colloidal quantum dot heterojunction. *Adv. Mater.* **2015**, *27*, 7445–7450. [CrossRef]
86. Xu, K.; Xiao, X.; Zhou, W.; Jiang, X.; Wei, Q.; Chen, H.; Deng, Z.; Huang, J.; Chen, B.; Ning, Z. Inverted Si:PbS colloidal quantum dot heterojunction-based infrared photodetector. *ACS Appl. Mater. Interfaces* **2020**, *12*, 15414–15421. [CrossRef]
87. Xiao, X.; Xu, K.; Yin, M.; Qiu, Y.; Zheng, L.; Cheng, X.; Yu, Y.; Ning, Z. High quality silicon: Colloidal quantum dot heterojunction based infrared photodetector. *Appl. Phys. Lett.* **2020**, *116*, 101102. [CrossRef]
88. Xu, Q.; Hu, J.; Wang, X. On-chip Ge, InGaAs, and colloidal quantum dot photodetectors: Comparisons for application in silicon photonics. *J. Opt. Soc. Am. B* **2021**, *38*, 194–200. [CrossRef]
89. Lin, Y.; Lee, K.H.; Son, B.; Tan, C.S. Low-power and high-detectivity Ge photodiodes by in-situ heavy As doping during Ge-on-Si seed layer growth. *Opt. Express* **2021**, *29*, 2940–2952. [CrossRef]
90. Zhu, J.; Zhu, H.; Liu, M.; Wang, Y.; Xu, H.; Ali, N.; Deng, H.; Tan, Z.; Cao, J.; Dai, N.; et al. Ultrabroadband and multiband infrared/terahertz photodetectors with high sensitivity. *Photonics Res.* **2021**, *9*, 2167–2175. [CrossRef]
91. Son, B.; Zhou, H.; Lin, Y.; Lee, K.H.; Tan, C.S. Gourd-shaped hole array germanium (Ge)-on-insulator photodiodes with improved responsivity and specific detectivity at 1,550 nm. *Opt. Express* **2021**, *29*, 16520–16533. [CrossRef]
92. Li, F.; Han, H.; Chen, Q.; Zhang, B.; Bao, H.; Dai, Y.; Ge, R.; Guo, S.; He, G.; Fei, Y.; et al. Saturation efficiency for detecting 1550 nm photons with a 2 × 2 array of $Mo_{0.8}Si_{0.2}$ nanowires at 2.2 K. *Photonics Res.* **2021**, *9*, 389–394. [CrossRef]
93. Yuan, Y.; Hyang, Z.; Zeng, X.; Liang, D.; Sorin, W.V.; Fiorentino, M.; Beausoleil, R.G. High Responsivity Si-Ge Waveguide Avalanche Photodiodes Enhanced by Loop Reflector. *IEEE J. Sel. Top. Quantum Electron.* **2022**, *28*, 3800508. [CrossRef]
94. Benedikovic, D.; Virot, L.; Aubin, G.; Hartmann, J.-M.; Amar, F.; Le Roux, X.; Alonso-Ramos, C.; Cassan, E.; Marris-Morini, D.; Boeuf, F.; et al. Silicon-Germanium Avalanche Receivers With fJ/bit Energy Consumption. *IEEE J. Sel. Top. Quantum Electron.* **2022**, *28*, 3802508. [CrossRef]

95. Pang, Y.; Liu, Z.; Liu, X.; Zhang, D.; Niu, C.; Li, M.; Zheng, J.; Zuo, Y.; Cheng, B. High-performance waveguide-coupled lateral Ge/Si avalanche photodetector. *Opt. Lett.* **2022**, *47*, 4463–4466. [CrossRef]
96. Benedikovic, D.; Virot, L.; Aubin, G.; Hartmann, J.-M.; Amar, F.; Le Roux, X.; Alonso-Ramos, C.; Cassan, E.; Marris-Morini, D.; Fedeli, J.-M.; et al. Silicon–germanium receivers for short-wave-infrared optoelectronics and communications. *Nanophotonics* **2021**, *10*, 1059–1079. [CrossRef]
97. Izhnin, I.I.; Lozovoy, K.A.; Kokhanenko, A.P.; Khomyakova, K.I.; Douhan, R.M.H.; Dirko, V.V.; Voitsekhovskii, A.V.; Fitsych, O.I.; Akimenko, N.Y. Single-photon avalanche diode detectors based on group IV materials. *Appl. Nanosci.* **2022**, *12*, 253–263. [CrossRef]
98. Wang, B.; Mu, J. High-speed Si-Ge avalanche photodiodes. *PhotoniX* **2022**, *3*, 8. [CrossRef]
99. Vines, P.; Kuzmenko, K.; Kirdoda, J.; Dumas DC, S.; Mirza, M.M.; Millar, R.W.; Paul, D.J.; Buller, G.S. High performance planar germanium-on-silicon single-photon avalanche diode detectors. *Nat. Commun.* **2019**, *10*, 1086. [CrossRef]
100. Llin, L.F.; Kirdoda, J.; Thorburn, F.; Huddleston, L.L.; Greener, Z.M.; Kuzmenko, K.; Vines, P.; Dumas DC, S.; Millar, R.W.; Buller, G.S.; et al. High sensitivity Ge-on-Si single-photon avalanche diode detectors. *Opt. Lett.* **2020**, *45*, 6406–6409. [CrossRef]
101. Das, R.; Xie, Y.; Frankis, H.; Chen, K.; Rufenacht, H.; Lamontagne, G.; Bradley JD, B.; Knights, A.P. Gain-enabled optical delay readout unit using CMOS-compatible avalanche photodetectors. *Photonics Res.* **2022**, *10*, 2422–2433. [CrossRef]
102. Marris-Morini, D.; Vakarin, V.; Ramirez, J.M.; Liu, Q.; Ballabio, A.; Frigerio, J.; Montesinos, M.; Alonso-Ramos, C.; Le Roux, X.; Serna, S.; et al. Germanium-based integrated photonics from near- to mid-infrared applications. *Nanophotonics* **2018**, *7*, 1781–1793. [CrossRef]
103. Koerner, R.; Fischer, I.A.; Schwarz, D.; Clausen, C.J.; Hoppe, N.; Schulze, J. Engineering of Germanium Tunnel Junctions for Optical Applications. *IEEE Photonics J.* **2018**, *10*, 2200912. [CrossRef]
104. Stepikhova, M.V.; Novikov, A.V.; Yablonskiy, A.N.; Shaleev, M.V.; Utkin, D.E.; Rutckaia, V.V.; Skorokhodov, E.V.; Sergeev, S.M.; Yurasov, D.V.; Krasilnik, Z.F. Light emission from Ge(Si)/SOI self-assembled nanoislands embedded in photonic crystal slabs of various periods with and without cavities. *Semicond. Sci. Technol.* **2019**, *34*, 024003. [CrossRef]
105. Peretokin, A.V.; Stepikhova, M.V.; Novikov, A.V.; Dyakov, S.A.; Zinovieva, A.F.; Smagina, Z.h.V.; Nasimov, D.A.; Rodyakina, E.E.; Zinovyev, V.A. Photonic crystal band structure in luminescence response of samples with Ge/Si quantum dots grown on pit-patterned SOI substrates. *Photonics Nanostruct.—Fundam. Appl.* **2023**, *53*, 101093. [CrossRef]
106. Stange, D.; Wirths, S.; Geiger, R.; Schulte-Braucks, C.; Marzban, B.; Von Den Driesch, N.; Mussler, G.; Zabel, T.; Stoica, T.; Hartmann, J.M.; et al. Optically pumped GeSn microdisk lasers on Si. *ACS Photonics* **2016**, *3*, 1279–1285. [CrossRef]
107. Al-Kabi, S.; Ghetmiri, S.A.; Margetis, J.; Pham, T.; Zhou, Y.; Dou, W.; Collier, B.; Quinde, R.; Du, W.; Mosleh, A.; et al. An optically pumped 2.5 μm GeSn laser on Si operating at 110 K. *Appl. Phys. Lett.* **2016**, *109*, 171105. [CrossRef]
108. Reboud, V.; Gassenq, A.; Pauc, N.; Aubin, J.; Milord, L.; Thai, Q.M.; Bertrand, M.; Guilloy, K.; Rouchon, D.; Rothman, J.; et al. Optically pumped GeSn micro-disks with 16% Sn lasing at 3.1 μm up to 180 K. *Appl. Phys. Lett.* **2017**, *111*, 092101. [CrossRef]
109. Savvin, A.; Dormidonov, A.; Smetanina, E.; Mitrokhin, V.; Lipatov, E.; Genin, D.; Potanin, S.; Yelisseyev, A.; Vins, V. NV—Diamond laser. *Nat. Commun.* **2021**, *12*, 7118. [CrossRef]
110. Wang, L.; Zhang, Y.; Sun, H.; You, J.; Miao, Y.; Dong, Z.; Liu, T.; Jiang, Z.; Hu, H. Nanoscale growth of a Sn-guided SiGeSn alloy on Si (111) substrates by molecular beam epitaxy. *Nanoscale Adv.* **2021**, *3*, 997. [CrossRef]
111. Lozovoy, K.A.; Kokhanenko, A.P.; Dirko, V.V.; Akimenko, N.Y.; Voitsekhovskii, A.V. Evolution of epitaxial quantum dots formed by Volmer–Weber growth mechanism. *Cryst. Growth Des.* **2019**, *19*, 7015–7021. [CrossRef]
112. Wang, S.; Zhang, N.; Chen, P.; Wang, L.; Yang, X.; Jiang, Z.; Zhong, Z. Toward precise site-controlling of self-assembled Ge quantum dots on Si microdisks. *Nanotechnology* **2018**, *29*, 345606. [CrossRef] [PubMed]
113. Dirko, V.V.; Lozovoy, K.A.; Kokhanenko, A.P.; Voitsekhovskii, A.V. Thickness-dependent elastic strain in Stranski–Krastanow growth. *Phys. Chem. Chem. Phys.* **2020**, *22*, 19318–19325. [CrossRef] [PubMed]
114. Liu, K.; Berbezier, I.; Favre, L.; Ronda, A.; Abbarchi, M.; Donnadieu, P.; Voorhees, P.W.; Aqua, J.-N. Capillary-driven elastic attraction between quantum dots. *Nanoscale* **2019**, *11*, 7798–7804. [CrossRef] [PubMed]
115. Lozovoy, K.A.; Zhou, Y.; Smith, R.; Lloyd, A.; Kokhanenko, A.P.; Dirko, V.V.; Akimenko, N.Y.; Grigoryev, D.V.; Voitsekhovskii, A.V. Thickness-dependent surface energy and formation of epitaxial quantum dots. *Thin Solid Film.* **2020**, *713*, 138363. [CrossRef]
116. Shklyaev, A.A.; Tsarev, A.V. Broadband Antireflection Coatings Made of Resonant Submicron- and Micron-Sized SiGe Particles Grown on Si Substrates. *IEEE Photonics J.* **2021**, *13*, 2200212. [CrossRef]
117. Nikiforov, A.; Timofeev, V.; Mashanov, V.; Azarov, I.; Loshkarev, I.; Volodin, V.; Gulyaev, D.; Chetyrin, I.; Korolkov, I. Formation of SnO and SnO_2 phases during the annealing of SnO(x) films obtained by molecular beam epitaxy. *Appl. Surf. Sci.* **2020**, *512*, 145735. [CrossRef]
118. Dirko, V.V.; Lozovoy, K.A.; Kokhanenko, A.P.; Voitsekhovskii, A.V. High-resolution RHEED analysis of dynamics of low-temperature superstructure transitions in Ge/Si(001) epitaxial system. *Nanotechnology* **2022**, *33*, 115603. [CrossRef]
119. Timofeev, V.; Mashanov, V.; Nikiforov, A.; Gutakovskii, A.; Gavrilova, T.; Skvortsov, I.; Gulyaev, D.; Firsov, D.; Komkov, O. Epitaxial growth of peculiar GeSn and SiSn nanostructures using a Sn island array as a seed. *Appl. Surf. Sci.* **2021**, *553*, 149572. [CrossRef]
120. Dirko, V.V.; Lozovoy, K.A.; Kokhanenko, A.P.; Kukenov, O.I.; Korotaev, A.G.; Voitsekhovskii, A.V. Peculiarities of the 7 × 7 to 5 × 5 superstructure transition during epitaxial growth of germanium on silicon (111) surface. *Nanomaterials* **2023**, *13*, 231. [CrossRef]

121. Rutckaia, V.; Heyroth, F.; Novikov, A.; Shaleev, M.; Petrov, M.; Schilling, J. Quantum dot emission driven by Mie resonances in silicon nanostructures. *Nano Lett.* **2017**, *17*, 6886–6892. [CrossRef]
122. Bai, X.; Purcell-Milton, F.; Gun'ko, Y.K. Optical Properties, Synthesis, and Potential Applications of Cu-Based Ternary or Quaternary Anisotropic Quantum Dots, Polytypic Nanocrystals, and Core/Shell Heterostructures. *Nanomaterials* **2019**, *9*, 85. [CrossRef] [PubMed]
123. de Mello Donegá, C. Synthesis and properties of colloidal heteronanocrystals. *Chem. Soc. Rev.* **2011**, *40*, 1512–1546. [CrossRef] [PubMed]
124. Zora, A.; Triberis, G.P.; Simserides, C. Near-Field Optical Properties of Quantum Dots, Applications and Perspectives. *Recent Pat. Nanotechnol.* **2011**, *5*, 188. [CrossRef] [PubMed]
125. Bera, D.; Qian, L.; Tseng, T.-K.; Holloway, P.H. Quantum Dots and Their Multimodal Applications: A Review. *Materials* **2010**, *3*, 2260–2345. [CrossRef]
126. Vukusic, L.; Kukucka, J.; Watzinger, H.; Milem, J.M.; Schaffler, F.; Katsaros, G. Single-shot readout of hole spins in Ge. *Nano Lett.* **2018**, *18*, 7141–7145. [CrossRef]
127. Watzinger, H.; Kukucka, J.; Vukusic, L.; Gao, F.; Wang, T.; Schaffler, F.; Zhang, J.-J.; Katsaros, G. A germanium hole spin qubit. *Nat. Commun.* **2018**, *9*, 3902. [CrossRef]
128. Hendrickx, N.W.; Lawrie WI, L.; Russ, M.; von Riggelen, F.; de Snoo, S.L.; Schouten, R.N.; Sammak, A.; Scappucci, G.; Veldhorst, M. A four-qubit germanium quantum processor. *Nature* **2021**, *591*, 580–585. [CrossRef]
129. Takeda, K.; Noiri, A.; Nakajima, T.; Kobayashi, T.; Tarucha, S. Quantum error correction with silicon spin qubits. *Nature* **2022**, *608*, 682–686. [CrossRef]
130. Warren, A.; Economou, S.E. Silicon qubits get closer to achieving error correction. *Nature* **2022**, *601*, 320–322. [CrossRef]